

## Contact metamorphism of the Black Hawk Zn-Pb-Cu deposit, Hancock County, Maine

Martin G. Yates  
and

Frank H. Howd

*Department of Geological Sciences, 110 Boardman Hall, University of Maine, Orono, Maine 04469*

*Date Received July 1, 1988*

*Date Accepted January 15, 1989*

The Black Hawk Zn-Cu-Pb deposit is located along the northern margin of the Sedgwick pluton within metasedimentary and metavolcanic rocks of the Ellsworth Schist. Most of the ores are composed of stratigraphically conformable, sphalerite-rich layers with locally high concentrations of galena, pyrite, pyrrhotite, and chalcopyrite. Galena-rich ores contain irregular intergrowths of tetrahedrite, bournonite, and boulangerite. The ore shows evidence of annealing and coarsening due to metamorphism.

The boundary between the Ellsworth Schist and the Sedgwick pluton is irregular due to the large number of granitic dikes emanating from the pluton. The Ellsworth Schist is regionally metamorphosed to the greenschist facies, and in the contact aureole of the pluton in the Black Hawk deposit schists contain cordierite and anthophyllite. A Si-poor, Mg-rich unit contains enstatite and spinel porphyroblasts in a fine-grained, massive talc, chlorite, and phlogopite groundmass. Sulfide-rich rocks contain phlogopite, magnesian chlorite, and rutile, reflecting high  $fS_2$  during metamorphism.

Metamorphic mineral assemblages along the Sedgwick pluton-Ellsworth Schist contact indicate contact metamorphism at pressures from 2.3 to 3.76 kbar (230-376 MPa) and at temperatures from 500-600°C. The magnesian metamorphic mineral assemblages result from combined effects of locally high  $fS_2$ - $fO_2$  conditions during metamorphism and early hydrothermal alteration associated with formation of the Zn-Pb-Cu deposits.

---

Le gisement de Zn-Cu-Pb de Black Hawk se situe le long de la bordure septentrionale du pluton de Sedgwick et est encaissé au sein des roches métasédimentaires et métavolcaniques du Schiste d'Ellsworth. La plupart des minerais se composent de couches riches en blende, en concordance dans l'ensemble stratifié et montrant localement des teneurs élevées en galène, pyrite, pyrrhotite et chalcopyrite. Les minerais riches en galène contiennent des plages irrégulières de tétrahédrite, bournonite et boulangerite. Le minerai porte la marque évidente d'une détrempe et d'une augmentation du grain dues au métamorphisme.

Le contact entre le Schiste d'Ellsworth et le pluton de Sedgwick est irrégulier par suite du grand nombre de dykes granitiques issus du pluton. Le Schiste d'Ellsworth a subi un métamorphisme régional dans le faciès des schistes verts; les schistes renferment de la cordiérite et de l'anthophyllite dans l'aurole de contact du pluton à l'intérieur du gisement de Black Hawk. Une unité pauvre en Si et riche en Mg montre des porphyroblastes d'enstatite et de spinelle au sein d'une fine mésostase massive composée de talc, chlorite et phlogopite. La présence de phlogopite, chlorite magnésienne et rutile dans les roches riches en sulfures trahit une  $fS_2$  élevée lors du métamorphisme.

Le long du contact entre le pluton de Sedgwick et le Schiste d'Ellsworth, les assemblages de minéraux métamorphiques mettent en évidence un métamorphisme de contact à des pressions de 2.3 à 3.76 kbar ainsi qu'à des températures de 500 à 600°C. Les assemblages de minéraux métamorphiques magnésiens proviennent de l'effet combiné de conditions de  $fS_2$ - $fO_2$  localement élevées et d'une altération hydrothermale précoce associée à la genèse des gisements de Zn-Pb-Cu.

[Traduit par le journal]

### INTRODUCTION

The Penobscot peninsula in southern Hancock County, Maine contains numerous small mines and prospects which have been developed sporadically since the late 1870s. The Black Hawk mine is the largest of 20 small prospects in the Second, Third, and Fourth Pond areas near Blue Hill which comprise the Blue Hill district. The Black Hawk mine lies beneath Second Pond, 3 km west of the town of Blue Hill (Fig. 1). The only other

commercially exploited deposit on the peninsula is located at the Harborside mine on Cape Rosier.

Exploration drilling at the Black Hawk property began prior to 1960, with attempts by the U.S. Bureau of Mines and Texas Gulf-Sulfur to discover a down-dip continuation of a series of small sulfide deposits exposed on the surface. In 1962, the Canadian-owned Black Hawk Mining Company took over development of the property. After additional drilling, they sank a shaft and began development on several levels. Following an

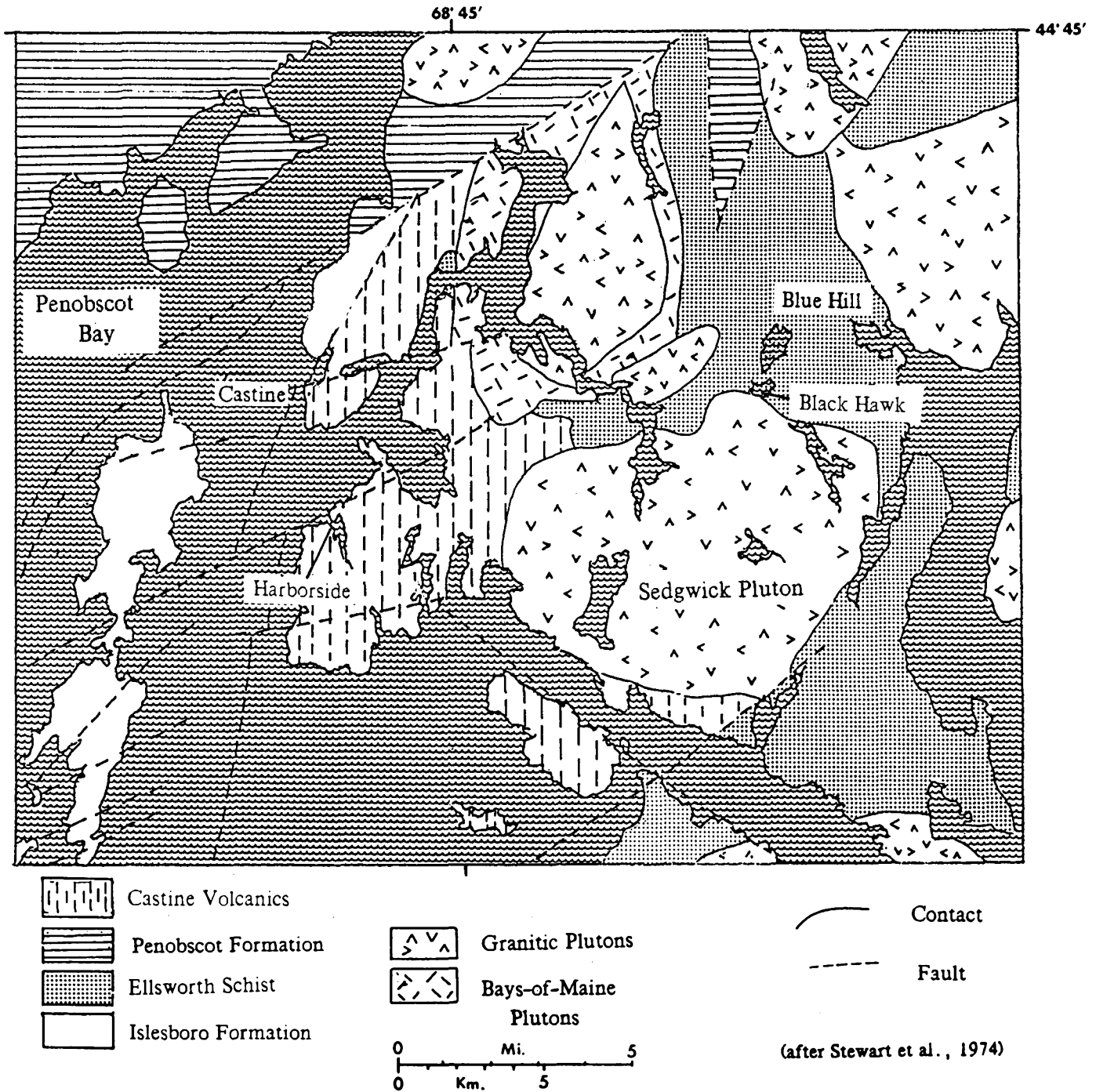


Fig. 1. Geologic map of Penobscot Peninsula, Hancock County, Maine showing the locations of the Black Hawk mine and the Harborside mine.

agreement between Black Hawk and Canadian-owned Kerr American Mining Limited, the latter continued the development of the Black Hawk mine in 1970 and operated the mine and mill until 1978.

Emmons (1909, 1910) published the first of several reports on the geology of the deposits in the Blue Hill district. He described the ores as pre-regional metamorphic, but Lindgren (1925), Newhouse and Flaherty (1930), and Li (1942) favored a contact metamorphic/replacement origin. More recent investigators, including Howd and Drake (1974) and Cheney (1969)

cited cross-cutting relationships between the sulfide and silicate phases as evidence for a hydrothermal/contact metamorphic origin of the deposits. However, Kinkel (1967) compared the characteristics of the Black Hawk ores with those of other Appalachian massive sulfide deposits, including those of New Brunswick. Like Emmons (1909), he concluded that the mineralization occurred prior to the intrusion of local granites, and that the sulfides were metamorphosed along with the enclosing strata. This conclusion was supported by LaPierre (1978) in his detailed investigation of the ores in the Black Hawk mine.

## REGIONAL GEOLOGY

The geology of the Penobscot peninsula was summarized by Cheney (1969), Stewart and Wones (1974), and Bouley (1978). The peninsula is composed of a series of metasedimentary and metavolcanic rocks cut by Devonian granitic plutons (Fig. 1). The Blue Hill district lies within the Ellsworth Schist, which is composed regionally of quartzo-feldspathic rocks, muscovite-chlorite schists, amphibolites, meta-quartzites, and felsic units. The Ellsworth Schist is unconformably overlain by the Late Silurian to Early Devonian Castine Volcanics which contains bimodal volcanic rocks, felsic tuffs, and volcano-clastic sedimentary rocks. The Ellsworth and Castine units were folded into large, southwest plunging, slightly overturned folds during Early Devonian time (Cheney, 1969). Both formations were contact metamorphosed by Devonian plutons to form biotite schist, hornfels, and quartzite.

The Ellsworth Schist is divided in the Black Hawk mine area into a number of distinct members (LaPierre, 1978). From bottom to top these members are the Douglas, Banded, and Pond quartzites, the Biotite schist, and the Allen quartzite. The ores are concentrated within the relatively clean, blue-gray to green-gray Pond quartzite and in isolated lenses within the light to medium gray, faintly banded Douglas quartzite. The Pond quartzite grades upward with increasing amounts of biotite into the Biotite

schist member. This member consists of finely interlayered, ribbon quartz- and biotite-rich layers which are strongly folded on a mesoscopic and microscopic scale. The Biotite schist member is overlain by the Allen quartzite which is a gray to purple, micaceous, cordierite-bearing quartzite.

The Ellsworth Schist dips to the southeast beneath the Sedgwick pluton at an angle of approximately 30°. All of the rocks within the mine area are cut by granitic sills and dikes which emanate from the Sedgwick pluton and which range in thickness from less than a meter to 60 m. In proximity to mineralized zones (LaPierre, 1978), the intrusions take on a distinctly green color due to the presence of amazonitic perthite.

The mineralization in the Black Hawk mine occurs in distinct zones within the Douglas and Pond quartzites separated by only sparsely mineralized or barren quartzite and schist (LaPierre, 1978). Mineralized zones can generally be divided into two types. The most extensive type of mineralization is concordant with enclosing strata, contains high concentrations of sphalerite with lesser amounts of chalcopryrite, pyrrhotite, and galena, and is hosted by both quartzite and massive, chloritic-phlogopitic rocks. The A Zinc Zone (Fig. 2) is of this type. The Lower Second Pond Copper Zone (50 m below the A Zinc Zone) contains chalcopryrite-pyrrhotite-pyrite mineralization which is concentrated into concordant bands. Like the concordant zinc-rich zones, these are most commonly hosted by quartzite. The

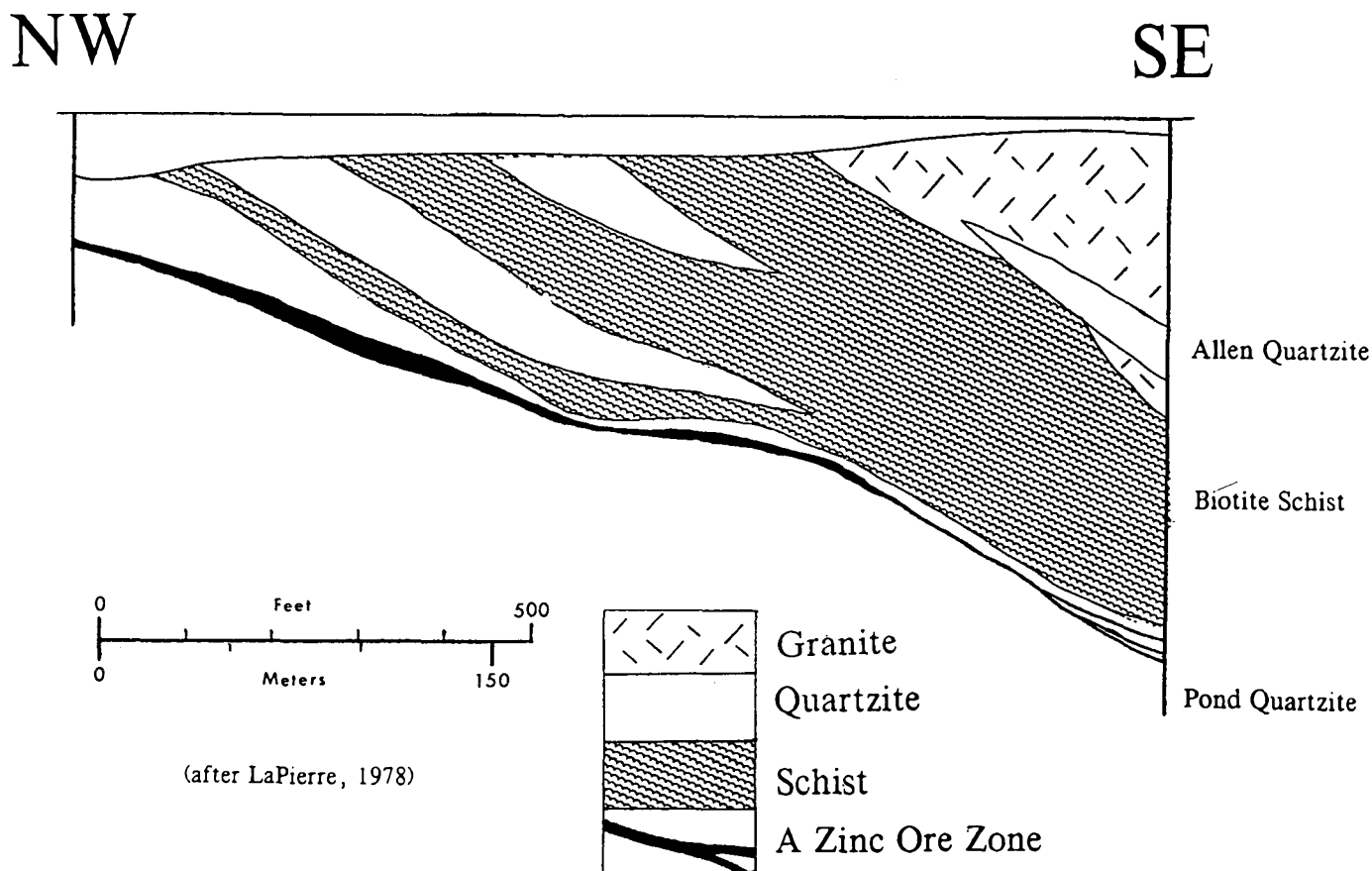


Fig. 2. Northwest to southeast geologic cross-section through the Black Hawk deposit showing the position of the A zinc ore zone.

other principal type of mineralization forms disseminated, irregular zones which are rich in pyrrhotite, pyrite, and chalcopyrite, and is hosted primarily by massive chloritic or phlogopitic rocks and less commonly by quartzite.

## MINERALOGY AND PETROLOGY

Because the underground workings of the Black Hawk mine are no longer open, samples collected during the operation of the mine and from small prospects on the surface and the dump have been used to provide insight into the nature of the ore and enclosing rocks. Samples BHE4, BHE15, BHRAD1, and BHRAD4, assemblages in which are analyzed in greatest detail below, were all derived from a 300 m x 200 m area in the underground workings near the A Zinc Zone approximately 300 m from the overlying Sedgwick pluton contact. The following generalizations were drawn on the basis of 60 polished blocks and 75 standard thin sections from the mine area.

### Sulfide Mineralogy

The Black Hawk mine sulfide mineralization listed in Table 1 is fairly simple and has been described previously by Li (1942) and LaPierre (1978) with the exception of the sulfosalts tetrahedrite, bourmonite, and boulangerite. The modal abundance of individual sulfides varies widely from sample to sample. Sphalerite, chalcopyrite, and pyrrhotite have the widest occurrence. Chalcopyrite is a ubiquitous minor constituent in sphalerite in the form of small rounded inclusions. Chalcopyrite also forms equant, rounded grains in polymineralic aggregates of sphalerite and pyrrhotite as well as pyrite and galena. Both monoclinic and hexagonal pyrrhotite polymorphs are present in mineralized samples. Monoclinic pyrrhotite is recognized in polished section as slightly lighter colored, higher relief fracture fillings and occasional irregular grains in hexagonal pyrrhotite. Monoclinic pyrrhotite is also recognized in X-ray powder patterns. The hexagonal form predominates and is commonly present without the monoclinic form.

Pyrite and galena have a more restricted occurrence in mineralized samples. Pyrite occurs primarily as irregular rounded grains in pyrrhotite in pyrrhotite-chalcopyrite-pyrite-rich ores. Pyrite grains include trails of small, rounded blebs of chalcopyrite, sphalerite, and galena. Euhedral cubes of pyrite are rare in most mineralized samples, although some skeletal remains suggest euhedral pyrite grains may once have been common. Pyrite hosted by quartzite develops smooth, rounded grains joined with quartz and other pyrite grains at triple junctions.

Anhedral masses of galena commonly serve as a matrix to other sulfide minerals and accompanying silicate and oxide minerals. While other sulfide minerals form coarse-grained polycrystalline aggregates, galena-rich samples characteristically contain poikiloblastic, crystallographically continuous domains of galena as large as 50 cm across. Galena is also a common constituent of amazonitic, granitic rocks, where it is in places finely disseminated around the periphery of amazonite grains. The sulfosalts tetrahedrite, bourmonite, and boulangerite, identified optically and with the microprobe, ap-

Table 1. Ore Mineralogy

Sphalerite	(Zn,Fe)S
Hex. Pyrrhotite	Fe <sub>1-x</sub> S
Mono. Pyrrhotite	Fe <sub>1-x</sub> S
Chalcopyrite	CuFeS <sub>2</sub>
Pyrite	FeS <sub>2</sub>
Galena	PbS
Tetrahedrite	(Cu,Ag) <sub>6</sub> (Cu,Fe,Zn) <sub>6</sub> (Sb,As,Bi) <sub>4</sub> S <sub>13</sub>
Bourmonite	CuPbSbS <sub>3</sub>
Boulangerite	Pb <sub>5</sub> Sb <sub>4</sub> S <sub>11</sub>

pear only in galena-rich samples and are intimately intergrown with galena. Figure 3A shows a grain of galena replaced by bourmonite along a chalcopyrite-galena grain boundary. Boulangerite forms euhedral blades and is associated with anhedral tetrahedrite, galena, and chalcopyrite masses (Fig. 3B).

The sulfide minerals vary texturally from strongly foliated and folded intergrowths to massive, porphyroblastic, or poikiloblastic intergrowths. Foliation and deformation are most easily observable in mineralogically banded ores. Chalcopyrite and pyrrhotite grains are elongated parallel to the direction of preferred orientation of enclosing and included chlorite and phlogopite grains. Pyrrhotite commonly develops a strong crystallographic preferred orientation in which its *c* axis is aligned with foliation. Other evidence of deformation includes brecciation and bending of included silicate grains. More commonly, sulfide mineral fabrics from the Black Hawk mine ores are massive and non-directed, and sulfides are intergrown in polycrystalline aggregates of rounded grains. Chalcopyrite and galena are usually interstitial to sphalerite and pyrrhotite. Pyrite, although usually anhedral and partially replaced, forms subhedral to euhedral porphyroblasts in massive ores.

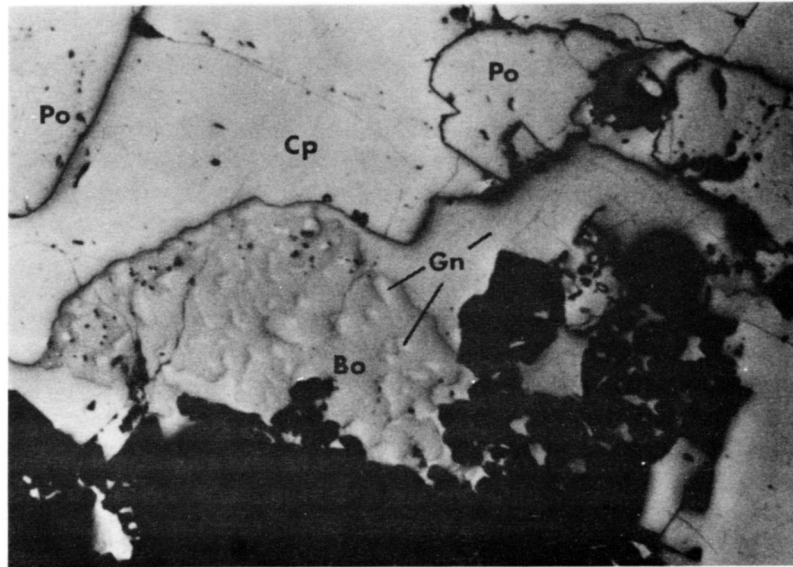
### Host Rock Mineralogy

Mineralized zones and enclosing strata in the Black Hawk mine contain a variety of metamorphic silicate and oxide mineral assemblages. A complete gradation from massive sulfide to finely disseminated sulfide is exhibited in the Black Hawk mine ores and the surrounding rocks. All of the local lithologic units contain sulfides, usually pyrrhotite or sphalerite, and their silicate and oxide mineralogies are strongly influenced as a result. Some mineralized strata are also rich in blue-green to brownish yellow, optically zoned tourmaline. Tourmaline from the Black Hawk mine has been examined in detail by Taylor and Slack (1984) who interpreted it to be recrystallized diagenetic tourmaline.

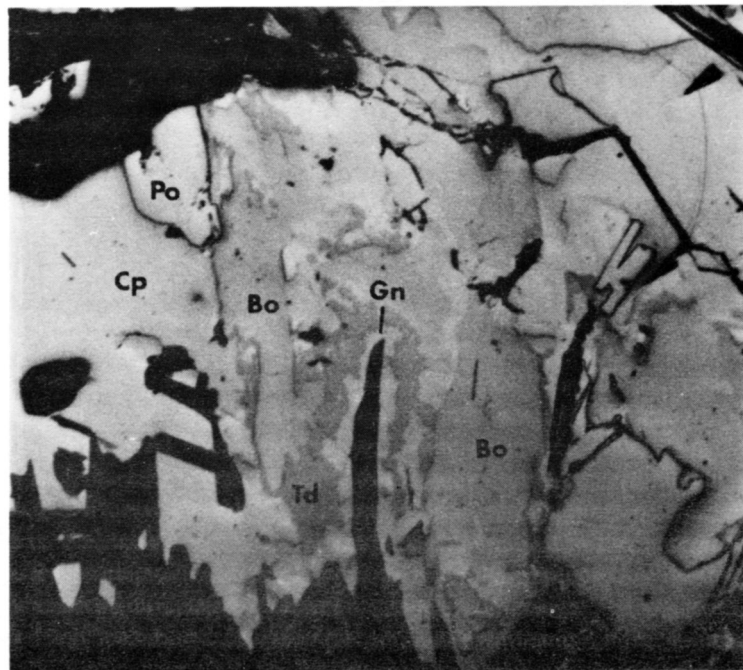
Cordierite is present throughout the contact metamorphosed pelitic rocks along with biotite, quartz, and rutile. Table 2 lists the two most common cordierite parageneses found in samples BHE4 and BHE15. The cordierite-anthophyllite assemblage (BHE4) has been described by Lindgren (1925) in the Blue Hill area and the cordierite-andalusite assemblage (BHE15) has been described by Gillson and Williams (1929) in contact metamor-

phic aureoles near Blue Hill. Biotite is present in both of these assemblages. It is commonly concentrated along the periphery of large cordierite poikiloblasts and throughout the intervening matrix, but is rarely included within cordierite. Quartz, rutile, zircon, magnetite, pyrite, and pyrrhotite are randomly scattered throughout both the cordierite-anthophyllite and cordierite-andalusite-bearing rocks. Rutile and zircon are present as stubby, prismatic crystals. Zircon grains included in cordierite have well-developed pleochroic halos and are generally more rounded

than rutile grains. Magnetite forms small, rounded grains, whereas pyrite and pyrrhotite are anhedral, irregular and always interstitial to silicate grains. Anthophyllite grains within BHE4 are well-formed, euhedral needles which are scattered either as individual grains or as radiating rosettes throughout the biotite-quartz-oligoclase matrix. Although anthophyllite is commonly in contact with the large cordierite poikiloblasts, like biotite, it is rarely included within cordierite (Fig. 3C). Andalusite in BHE15 forms anhedral masses, which are elongated along foliation.

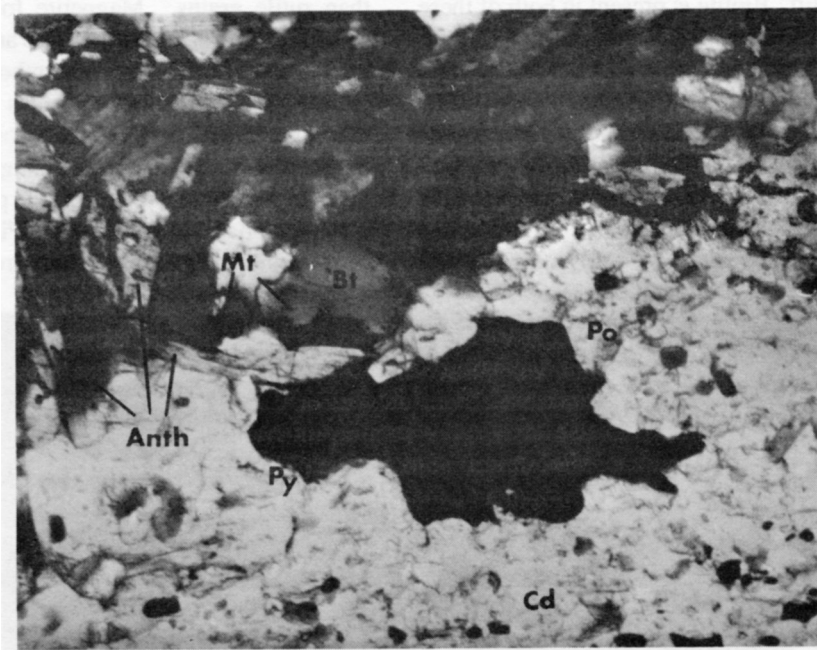


a

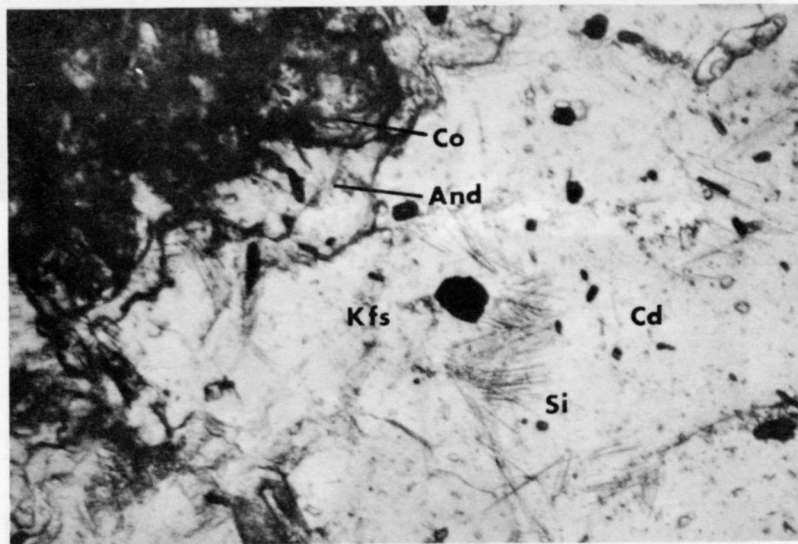


b

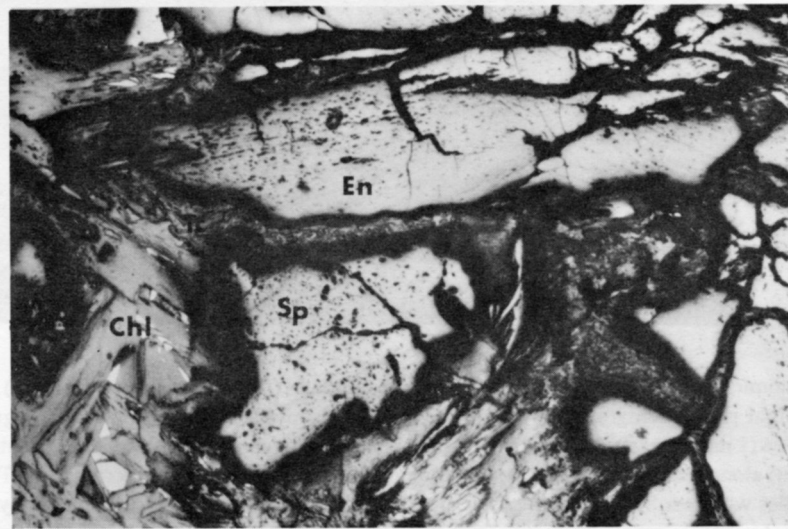
Fig. 3 (a) Reflected-light photomicrograph of galena (Gn) replaced by boumonite (Bn) along chalcopyrite (Cp) grain boundary in BHRAD5a (0.5 mm across). (b) Reflected-light photomicrograph showing intergrown chalcopyrite (Cp), pyrrhotite (Po), galena (Gn), tetrahedrite (Td), and boulangierite (Bo) in BHRAD5a (1 mm across). (c) Transmitted-light photomicrograph showing biotite (Bt), anthophyllite (Anth), magnetite (Mt), pyrite (Py), and pyrrhotite (Po) along the edge of a cordierite (Cd) poikiloblast in BHE4 (1.1 mm across). (d) Transmitted-light photomicrograph showing sillimanite (Si) needles within orthoclase (Kfs) and cordierite (Cd) next to corundum (Co) armored by andalusite (And) in BHE15 (0.52 mm across). (e) Reflected-light photomicrograph showing enstatite (En) and spinel (Sp) separated by retrograde talc (Tc) bordered by massive chlorite (Chl) in BHRAD1 (1.5 mm across). (f) Reflected-light photomicrograph showing enstatite (En), spinel (Sp), and forsterite (Fo) with interstitial chlorite (Chl) and phlogopite (Phl) in BHRAD4 (1.3 mm across).



c



d



e

Fig. 3 Cont.

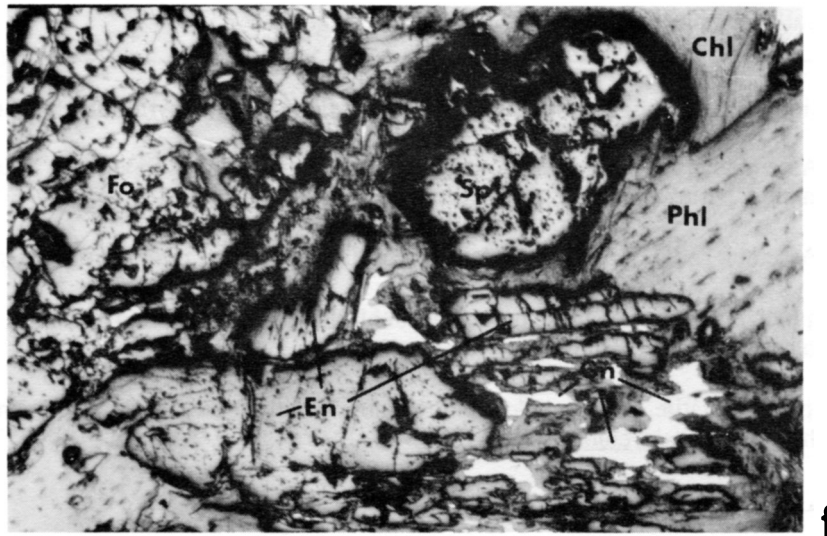


Fig. 3 Cont.

BHE15 also contains sillimanite needles intergrown with orthoclase (microperthite) and cordierite (Fig. 3D). Corundum is present in BHE15 (Assemblage B) where it is armored by andalusite, cordierite, and retrograde muscovite and includes grains of gahnite, rutile, and sulfide. Corundum has also been described in the Blue Hill area by Gillson and Williams (1929).

Strongly mineralized zones are found in both the cordierite-andalusite and cordierite-anthophyllite-bearing rocks, but sulfide mineralization is more commonly hosted by unusually Si-poor, Mg-Al-rich rocks composed of chlorite and phlogopite with varying amounts of amphibole, enstatite, spinel, and olivine. These lithologies were referred to as radiating amphibolite dikes (RAD) as the Black Hawk mine was being developed. The name reflects the radiating intergrowth of amphibole prisms discovered in drill core. However, LaPierre (1978) found no cross-cutting or intrusive contacts associated with the RAD units. He described some RAD lithologies as roughly conformable with bedding and strongly associated with mineralization.

Mineral assemblages for samples BHRAD1 and BHRAD4 are listed in Table 2. Both contain coarse, equant porphyroblasts of clear to slightly green spinel and coarse, prismatic enstatite crystals in a matrix of randomly oriented chlorite, phlogopite, and talc (Fig. 3E). BHRAD1 contains elongated, prismatic tremolitic hornblende crystals and subordinate quantities of phlogopite compared to chlorite. BHRAD4 is phlogopite-rich and contains coarse, rounded, slightly elongated grains of forsterite (Fig. 3F). Unlike chlorite in BHRAD1, chlorite in BHRAD4 is minor and is restricted to fine-grained intergrowths with talc. It is therefore interpreted as secondary in BHRAD4. Both BHRAD1 and BHRAD4 are rich in pyrrhotite and galena. Sphalerite and pyrite, although present in some RAD occurrences, are absent in these two samples.

#### ANALYTICAL METHOD

Mineral chemistry of silicates was determined through the use of the University of Maine's MAC 400S electron microprobe equipped with three wavelength dispersive spectrometers and

Krisel automation. The analyses were performed using natural and synthetic, silicate and oxide standards of simple composition. The raw X-ray counts were corrected for absorption and fluorescence using the correction scheme of Bence and Albee (1968). All analyses were conducted using an accelerating potential of 15 kV, a beam current of 0.02 or 0.03  $\mu$ A, 50000 count or 20 sec maximums, and a spot size of approximately 4  $\mu$ m. Standardizations were routinely checked by analyzing mineral standards.

#### MINERAL CHEMISTRY

The average chemical compositions of selected minerals from rocks enclosing Black Hawk mine ores are listed in Table 3 and individual mineral analyses are shown diagrammatically in Figures 4 and 5. The large variations in mineral composition (particularly Fe/(Fe+Mg)) are related to variations in mode and mineralogy within the suite of samples. Biotite compositions range from near Mg-end-member phlogopite in BHRAD4 to more intermediate biotites in samples BHE4 and BHE15. Manganese is present in biotites from all three samples and reaches 0.44% MnO in BHE15. The alumina content in biotite is also highest in BHE15, which reflects alumina saturation in the presence of andalusite and corundum. The Na-content of the highly magnesian biotites in BHRAD4 is well above that of the biotites in BHE4 and BHE15. Similar Na-rich biotites have been described in highly magnesian assemblages of Sar-e-Sang, Afghanistan (Grew, 1988).

The biotite-cordierite  $K_D$  of 0.47 and 0.46 in BHE4 and BHE15, where  $K_D = (Mg/Fe)^{Crd}/(Mg/Fe)^{Bt}$ , are within one standard deviation of experimentally determined  $K_D$ 's of Holdaway and Lee (1977). The anthophyllite-cordierite  $K_D$  calculated for BHE4 is 2.311, where  $K_D = (Mg/Fe)^{Crd}/(Mg/Fe)^{Anth}$ , which compares favorably with observed  $K_D$ 's of Lal and Moorehouse (1969), Bachinski (1976), and Blümel and Propach (1978).

The Fe/(Fe+Mg) ratio and MnO-content of cordierite in sample BHE15 are slightly higher than cordierite in BHE4. Figure 4 shows that the cordierite in BHE15 is also slightly more

Table 2. Mineral Assemblages

BHE4	Biotite, quartz, oligoclase, anthophyllite, cordierite, pyrite, pyrrhotite, magnetite.
BHE15	(Assemblage A) Cordierite, biotite, andalusite, orthoclase microperthite, sillimanite, rutile, gahnite, pyrite, sphalerite, pyrrhotite, chalcopyrite, <u>muscovite</u> , <u>chlorite</u> .  (Assemblage B) Corundum, andalusite, cordierite, gahnite, rutile, pyrite, <u>muscovite</u> .
BHRAD1	Spinel, enstatite, tremolitic hornblende, chlorite, phlogopite(minor), zircon, rutile, pyrrhotite, galena, <u>talc</u> and <u>chlorite</u> .
BHRAD4	Spinel, enstatite, olivine, phlogopite, tremolitic hornblende, pyrrhotite, galena, boulangerite, chalcopyrite, <u>talc</u> , <u>chlorite</u> .  ... <u>Secondary</u>

aluminous than in BHE4, which, like the biotite compositions, is consistent with the presence of corundum and andalusite in BHE15. Cordierites in BHE15 are also more Mn-rich than those of BHE4. This parallels the enrichment of Mn in biotite in BHE15 over those in BHE4.

Anthophyllite from BHE4 shows only a slightly higher Fe/(Fe+Mg) than coexisting biotite but is well above that of coexisting cordierite. A trend of increasing iron content from cordierite, through biotite, to anthophyllite is well known in metamorphosed sulfide deposits (Wolter and Seifert, 1984) and suggests an equilibrium Fe-Mg distribution.

The Si-deficient, Mg-enriched samples BHRAD1 and BHRAD4 both contain enstatite with low Fe/(Fe+Mg) and high Al. The Fe/(Fe+Mg) content of enstatite is intermediate with respect to co-existing forsterite and spinel. Differences between the average alumina contents of enstatite in the forsterite-present (BHRAD4) and forsterite-absent (BHRAD1) assemblages are insignificant (Table 3). Individual spinel grains intergrown with forsterite tend to be slightly more magnesian than those associated with enstatite alone (Fig. 5). Spinel is the non-sulfide phase most enriched in iron in both BHRAD1 and BHRAD4, which is in part due to ferric iron. Of the non-sulfide minerals in BHRAD1 and BHRAD4 only spinel incorporates significant amounts of Zn. However, true gahnite is present only in samples bearing sphalerite (e.g., BHE15).

Clinoamphibole is the only Ca-bearing phase in either BHRAD1 or BHRAD4. Like the other non-sulfide minerals, the clinoamphibole is close to the magnesian end-member. It also contains more alumina than the tremolite end-member, thus falling in the compositional range of tremolitic hornblende (Hawthorne, 1981).

## DISCUSSION

### P-T-X Relations

The phase relations among the silicates in the Black Hawk mine ores reflect high temperatures and low pressures indicative of contact metamorphism as has been previously noted by

Gillson and Williams (1929) and Cheney (1969). Figure 6 shows pertinent univariant equilibria in pressure-temperature space for the system MgO-Al<sub>2</sub>O<sub>3</sub>-SiO<sub>2</sub>-H<sub>2</sub>O (MASH), with several equilibria from the system K<sub>2</sub>O-MgO-Al<sub>2</sub>O<sub>3</sub>-SiO<sub>2</sub>-H<sub>2</sub>O (KMASH) superimposed. The positions of some of these equilibria were calculated from the internally consistent data base of Berman *et al.* (1986) and the method of Perkins *et al.* (1986) using the program GE0CALC. All equilibria calculations involve stoichiometric end-member phases (except cordierite and enstatite) and assume  $P_T = P_{H_2O}$ . Solution of alumina in enstatite in the presence of spinel and solution of water in cordierite are incorporated in the GE0CALC database (Berman *et al.*, 1986).

Andalusite is the most abundant aluminosilicate in the Blue Hill area, which indicates pressures less than 3.76 kbar (376 MPa) (aluminosilicate triple point, Holdaway, 1971). However, fibrolitic sillimanite is reported around the northern perimeter of the Sedgwick pluton (Cheney, 1969) and appears intergrown with cordierite and microperthite in BHE15. The growth of sillimanite in the presence of K-feldspar requires higher temperatures than the muscovite + quartz = sillimanite + K-feldspar + H<sub>2</sub>O equilibria on Figure 6.

The presence of cordierite and anthophyllite in magnesian rocks such as BHE4 is a common feature in low-pressure, high-temperature metamorphic terrains, particularly in rocks containing sulfides, e.g., Falun, Sweden (Wolter and Seifert, 1984), Bodenmais, E. Bavaria (Blümel and Propach, 1978), Notre Dame Bay, Newfoundland (Bachinski, 1976), Gullbridge, Newfoundland (Upadhyay and Smitheringale, 1972), the Ambaji and Deri deposits, India (Deb, 1980), and the Coronation deposit, Saskatchewan (Froese, 1969). Cordierite-anthophyllite is chemically equivalent with the lower temperature assemblage quartz-chlorite. The upper temperature stability of quartz + chlorite is determined experimentally by Fleming and Fawcett (1976) and Chernosky (1978). They suggested that the upper temperature stability of quartz + chlorite is independent of iron or alumina content of the system, although the high temperature assemblages may vary. Figure 6 shows the reaction clinocllore + quartz = anthophyllite + cordierite + H<sub>2</sub>O lies close to the muscovite + quartz = aluminosilicate + K-feldspar + H<sub>2</sub>O uni-

Table 3. Representative mineral chemistries, Black Hawk mine.

Mineral	Biotite			Anthophyllite		Cordierite		Enstatite		Forsterite	Spinel			Chlorite	Amphibole
	BHE4	BHE15	BHRAD4	BHE4	BHE4	BHE15	BHRAD1	BHRAD4	BHRAD4	BHRAD1 <sup>1</sup>	BHE15 <sup>1</sup>	BHRAD4 <sup>1</sup>	BHRAD1	BHRAD1	
Sample	BHE4	BHE15	BHRAD4	BHE4	BHE4	BHE15	BHRAD1	BHRAD4	BHRAD4	BHRAD1 <sup>1</sup>	BHE15 <sup>1</sup>	BHRAD4 <sup>1</sup>	BHRAD1	BHRAD1	
SiO <sub>2</sub>	39.14	37.76	44.75	53.95	48.71	48.83	55.31	55.10	41.31	nd.	nd.	nd.	31.47	54.00	
TiO <sub>2</sub>	2.28	2.00	1.02	0.10	0.02	0.30	0.10	0.09	0.21	0.00	0.30	0.06	0.15	0.40	
Al <sub>2</sub> O <sub>3</sub>	15.72	16.80	13.91	1.77	33.45	33.98	4.17	4.23	0.19	67.75 <sup>2</sup>	57.47 <sup>2</sup>	68.69 <sup>2</sup>	21.23	5.59	
Fe <sub>2</sub> O <sub>3</sub>	nd.	nd.	nd.	nd.	nd.	nd.	nd.	nd.	nd.	1.39 <sup>2</sup>	0.91 <sup>2</sup>	1.43 <sup>2</sup>	nd.	nd.	
FeO <sup>T</sup>	13.52	13.82	0.98	19.02	4.23	4.15	3.40	4.51	3.87	4.87 <sup>2</sup>	7.75 <sup>2</sup>	3.26 <sup>2</sup>	2.05	1.86	
MnO	0.17	0.44	0.13	1.08	0.34	1.14	0.35	0.37	0.81	0.26	0.67	0.33	0.10	0.52	
ZnO	nd.	nd.	nd.	nd.	nd.	nd.	0.07	0.01	nd.	3.34	29.87	1.79	nd.	0.05	
HgO	16.68	15.69	24.91	21.50	11.93	10.12	35.60	35.39	53.65	22.59	3.42	24.58	31.29	22.53	
CaO	nd.	nd.	nd.	0.12	0.01	0.31	0.06	0.11	0.00	nd.	nd.	nd.	nd.	11.72	
Na <sub>2</sub> O	0.61	0.07	1.16	0.21	0.42	0.14	nd.	nd.	nd.	nd.	nd.	nd.	nd.	0.64	
K <sub>2</sub> O	8.11	9.56	8.04	0.01	0.01	0.05	nd.	nd.	nd.	nd.	nd.	nd.	nd.	0.05	
Total	96.23	96.14	94.90	97.76	98.22	98.42	100.06	99.91	100.04	100.20	100.09	100.14	86.29	97.37	
	Cations and Number of Oxygens														
Oxygens	22	22	22	23	18	18	6	6	4	Normalized to 3 Cations			28	23	
Si	5.681	5.549	6.155	7.736	4.946	4.954	1.915	1.391	0.988	-	-	-	5.908	7.423	
Al	2.319	2.451	1.845	0.264	1.054	1.046	0.085	0.109	0.005	-	-	-	2.092	0.577	
Total	8.000	8.000	8.000	8.000	6.000	6.000	2.000	2.000	0.993	0.000	0.000	0.000	8.000	8.000	
Ti	0.249	0.221	0.106	0.011	0.002	0.000	0.003	0.002	0.004	0.000	0.000	0.001	0.021	0.041	
Al	0.370	0.459	0.410	0.035	2.949 <sup>3</sup>	3.017 <sup>3</sup>	0.082	0.062	-	1.974	1.980	1.974	2.605	0.329	
Fe <sup>+++</sup>	-	-	-	-	-	-	-	-	-	0.026	0.020	0.026	-	-	
Fe <sup>++</sup>	1.641	1.698	0.113	2.281	0.359	0.352	0.097	0.132	0.077	0.101	0.190	0.056	0.322	0.214	
Mn	0.021	0.055	0.015	0.131	0.029	0.098	0.002	0.000	0.016	0.061	0.645	0.032	0.016	0.005	
Zn	-	-	-	-	-	-	0.010	0.011	-	0.005	0.017	0.007	-	0.061	
Hg	3.609	3.437	5.108	4.596	1.670	1.530	1.804	1.810	1.914	0.833	0.149	0.893	8.757	4.617	
Total	5.890	5.870	5.752	7.054	5.009	4.997	1.998	2.197	-	3.000	3.000	3.000	11.721	5.268	
Ca	-	-	-	0.018	0.001	0.001	0.002	0.004	0.000	-	-	-	-	1.726	
Na	0.172	0.020	0.309	0.058	0.383	0.028	-	-	-	-	-	-	-	0.171	
K	1.502	1.793	1.411	0.002	0.001	0.006	-	-	-	-	-	-	-	0.009	
Total	1.674	1.813	1.720	0.078	0.085	0.035	0.002	0.004	2.011	0.000	0.000	0.000	0.000	1.906	
Total Cations	15.564	15.683	15.472	15.133	11.093	11.032	4.000	4.021	3.004	3.000	3.000	3.000	19.722	15.173	
Fe/(Fe+Mg)	0.313	0.331	0.025	0.332	0.177	0.187	0.051	0.068	0.039	<sup>4</sup> 0.132 <sup>5</sup> 0.107	<sup>4</sup> 0.585 <sup>5</sup> 0.560	<sup>4</sup> 0.093 <sup>5</sup> 0.059	0.035	0.044	

<sup>1</sup>CR and V below detection<sup>2</sup>Calculated value assuming 3 Cations<sup>3</sup>Al(IV)<sup>4</sup>Calculated using FeO<sup>T</sup><sup>5</sup>Calculated using FeO

nd.- Element not determined.

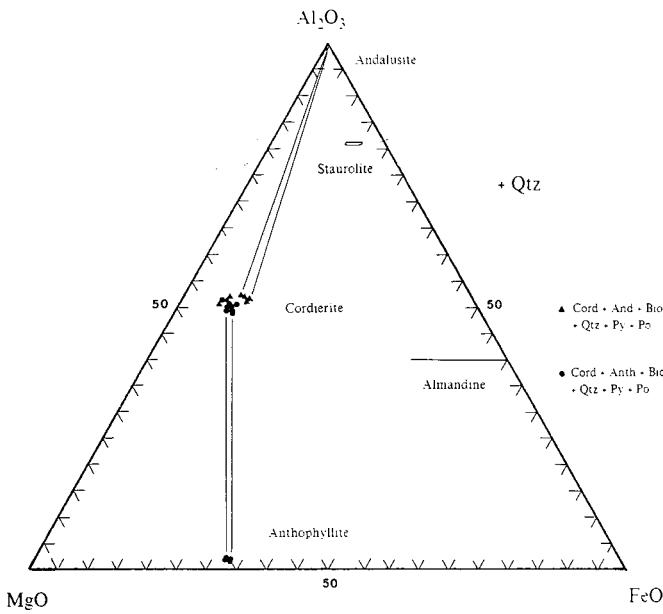


Fig. 4. AFM diagram with cordierite and anthophyllite compositions and coexisting mineral assemblages. Filled triangles indicate sample BHE4; filled circles indicate sample BHE15. Tie lines indicate grain to grain contact.

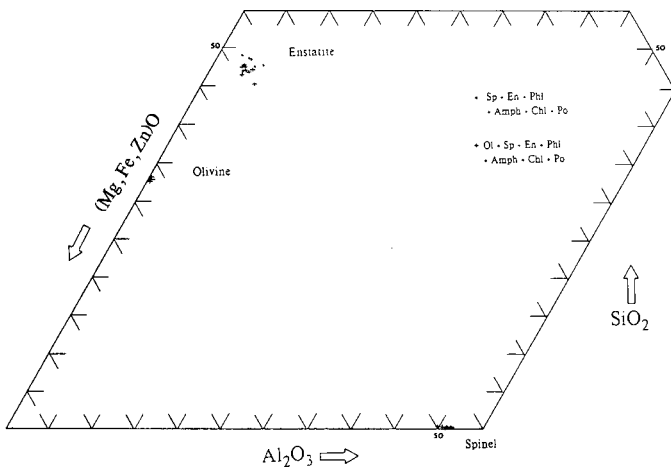


Fig. 5. Partial (Mg,Fe,Zn)O-Al<sub>2</sub>O<sub>3</sub>-SiO<sub>2</sub> diagram with olivine, enstatite, and spinel compositions and coexisting mineral assemblages. Solid dots indicate sample BHRAD1; Cross marks indicate sample BHRAD4.

variant line in the 2 to 4 kbar (200 to 400 MPa) range. The minimum temperature of the cordierite-anthophyllite assemblage under  $P_T = P_{H_2O}$  conditions increases from 590° to 630°C as pressure increases from 2 to 3.76 kbar (200 to 376 MPa).

The upper temperature limits of the rocks in the Black Hawk mine area are constrained primarily by the assemblages observed in the SiO<sub>2</sub>-poor, MgO-enriched rocks accompanying mineralization. Both BHRAD1 and BHRAD4 have high temperature assemblages containing spinel + enstatite + amphibole + phlogopite + chlorite ± forsterite. Fine-grained chlorite and talc are always present along intergranular boundaries in these magnesian assemblages and are interpreted as retrograde replacements. However, some coarse, bladed chlorite grains in BHRAD1 may be primary. They are uniform in composition and in some cases

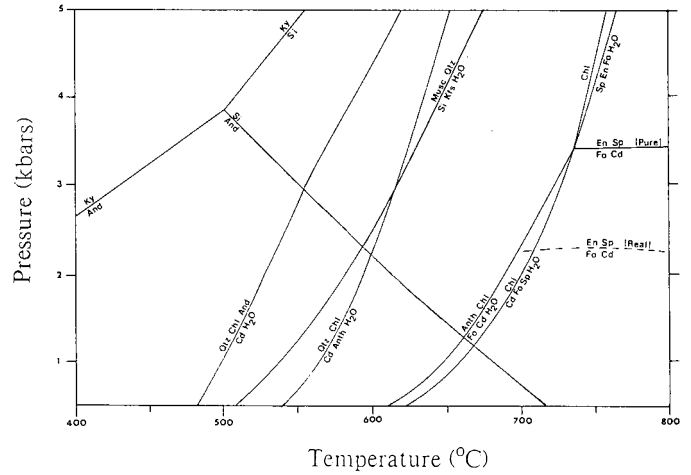


Fig. 6. Pressure vs. temperature diagram for selected equilibria in the system K<sub>2</sub>O-MgO-Al<sub>2</sub>O<sub>3</sub>-SiO<sub>2</sub>-H<sub>2</sub>O. The diagram is constructed using GEOCALC (Berman *et al.*, 1986; Perkins *et al.*, 1986) for  $P_T = P_{H_2O}$ . (See text for details).

include or partially include grains of enstatite and spinel. Textural equilibrium intergrowth of the enstatite, spinel, and forsterite is rare due to retrograde effects, but the grains are commonly separated only by a few microns. Further evidence for the equilibrium between spinel, enstatite, and forsterite is the trend of increasing Fe/(Fe+Mg): forsterite < enstatite < spinel. Identical trends of iron enrichment were reported from a kornepurine-magnesite-phlogopite rock associated with white schists (Grew, 1988) and in contact metamorphosed peridotites (Frost, 1976).

The persistence of chlorite and the development of an equilibrium enstatite + spinel + forsterite assemblage suggests P-T conditions close to the clinoclone = forsterite + enstatite + spinel + H<sub>2</sub>O univariant line of Figure 6. This chlorite breakdown reaction and the corresponding lower pressure chlorite breakdown reaction of chlorite = forsterite + cordierite + spinel + H<sub>2</sub>O have been studied experimentally by Fawcett and Yoder (1966).

The assemblage cordierite + forsterite is not present in any of the magnesian samples from the Black Hawk mine, which suggests P-T conditions on the high-pressure side of the nearly isobaric reaction enstatite + spinel = forsterite + cordierite. However, the position of this line is shifted to lower pressures with the addition of small amounts of iron in the participating phases (Frost, 1976). Figure 6 shows the effect of decreased enstatite, spinel, forsterite, and cordierite activity on the enstatite + spinel = forsterite + cordierite equilibria. The activities of enstatite, spinel, and forsterite correspond to Fe/(Fe+Mg) values listed for BHRAD4 in Table 3. The Fe/(Fe+Mg) for cordierite is calculated from the cordierite-orthopyroxene  $K_D$  of Frost (1975). The adjusted pressure of the enstatite + spinel = forsterite + cordierite equilibria decreases from 3.4 kbar to 2.3 kbar (340 to 230 MPa). This pressure shift may be exaggerated due to its large dependence on the activity of enstatite.

The position of the chlorite-out univariant curve in Figure 6 places an upper temperature limit on the magnesian assemblages of 700° at 2.3 kbar (230 MPa) to 730° at 3.76 kbar (376 MPa) assuming  $P_T = P_{H_2O}$  conditions. This places metamorphic conditions well within the sillimanite field, which is contrary to metamorphic conditions suggested by more abundant andalusite.

The activity of water in a contact metamorphic aureole of a relatively dry granitic melt is likely to be less than unity, particularly in the presence of abundant sulfide minerals where significant quantities of  $\text{SO}_2$  and  $\text{H}_2\text{S}$  may be present (Bachinski, 1976). The effect of decreased water activity on the dehydration reactions in Figure 6 is a shift toward lower temperatures at a particular pressure. The dominance of andalusite and rare development of fibrolitic sillimanite as in sample BHE15 suggest that metamorphic temperatures could not have greatly exceeded the andalusite field of stability and suggests temperatures near 500-600°C. However, the close proximity to the Sedgwick pluton and the abundance of granitic dikes and sills would lead to temperature gradients even within the restricted area in the A Zinc Zone from which the samples were collected.

### Sulfide-Silicate Relations

The cordierite-anthophyllite-biotite and spinel-enstatite-forsterite parageneses at Blue Hill are depleted in FeO because of elevated  $f_{\text{S}_2}$  values due to the high concentration of sulfides. The effect of fluctuating  $f_{\text{O}_2}$  and  $f_{\text{S}_2}$  in the fluid on the FeO contents in silicate and oxide phases has been demonstrated by numerous researchers (e.g., Guidotti, 1970; Thompson, 1972; Bachinski, 1976; Froese, 1969) and can be calculated through methods outlined by Froese (1971 and 1976) and Nesbitt (1986). Figure 7 is an  $f_{\text{O}_2}$ - $f_{\text{S}_2}$  diagram for the system Fe-Ti-O-S with superimposed  $X_{\text{Fe}}$  isopleths in biotite for 600°C and  $P_{\text{H}_2\text{O}}=3$  kbar (300 MPa) metamorphic conditions. Equilibria among the minerals in the Fe-Ti-O-S system are calculated at P and T using thermodynamic data from Robie *et al.* (1978). The activity of FeS is corrected for variations T, P, and  $f_{\text{S}_2}$  after the method of Froese and Gunter (1976), using experimental data of Toulmin and Barton (1964). The  $X_{\text{Fe}}$  biotite isopleths are calculated through reactions such as  $\text{Ann} + \text{S}_2 = \text{Po} + \text{Kfs} + \text{H}_2\text{O}$  and  $\text{Ann} + \text{O}_2 = \text{Mte} + \text{Kfs} + \text{H}_2\text{O}$  in each of the iron oxide and sulfide fields using equilibrium constants calculated from Nesbitt (1986) and adjusted to P and T using the equations of Slaughter *et al.* (1975).

Pyrrhotite is present in all sulfide assemblages in the Black Hawk mine deposit and is accompanied by pyrite and magnetite in many assemblages. The presence of magnetite, pyrrhotite, and pyrite indicates buffered  $f_{\text{O}_2}$ - $f_{\text{S}_2}$  conditions near the triple point at  $f_{\text{O}_2}=-16.1$  and  $f_{\text{S}_2}=-1.9$  (Fig. 7). The widespread occurrence of rutile in the ores also indicates relatively high metamorphic  $f_{\text{O}_2}$  or  $f_{\text{S}_2}$  conditions. The ilmenite-rutile phase boundary in Figure 7 was calculated using pure  $\text{FeTiO}_3$ .  $\text{Fe}^{3+}$  in ilmenite would expand the ilmenite field and elevate the lower  $f_{\text{O}_2}$  and  $f_{\text{S}_2}$  limits in the pyrrhotite and magnetite fields.

The mole fraction of annite in biotite in the presence of potassium feldspar at 600°C and 3 kbar (300 MPa) is fixed at a value of 0.146 at the magnetite-pyrite-pyrrhotite triple point and drops sharply along the pyrrhotite-pyrite join. However, annite contents of biotite in BHE4 and BHE15 are 0.313 and 0.331, respectively. The  $K_D$ 's measured between biotite, cordierite, and anthophyllite in BHE4 and BHE15 are not inconsistent with equilibration at a temperature below 600°C, as the biotite-cordierite  $K_D$  is relatively temperature-insensitive (Holdaway and Lee, 1977). The  $f_{\text{O}_2}$ - $f_{\text{S}_2}$  position of the magnetite-pyrite-

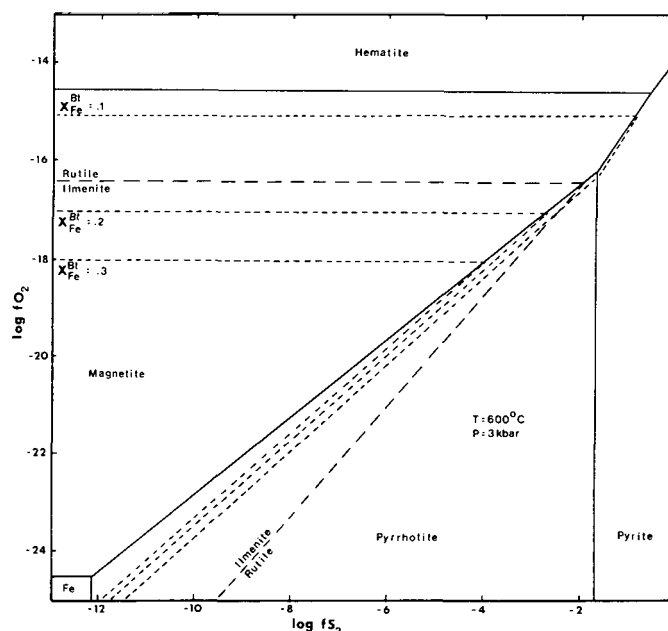


Fig. 7. Log  $f_{\text{O}_2}$  vs. log  $f_{\text{S}_2}$  diagram for the system Fe-Ti-O-S constructed at 600°C and  $P_{\text{T}}=P_{\text{H}_2\text{O}}=3$  kbar. Short dashed lines indicate mole fraction of annite in biotite assuming the presence of K-feldspar.

pyrrhotite triple point is much more sensitive to temperature. At 3 kbar (300 MPa) and temperatures below 560°C the annite content of biotite could exceed 0.3. Increased pressure would have a smaller effect on the position of the  $f_{\text{O}_2}$ - $f_{\text{S}_2}$  triple point but would favor annite through the reaction:  $\text{Ann} + \text{O}_2 = \text{Mte} + \text{Kfs} + \text{H}_2\text{O}$ . Consequently, the anomalously high iron content of the  $f_{\text{O}_2}$ - $f_{\text{S}_2}$  buffered biotites may reflect either lower temperature or higher pressure than was assumed in constructing Figure 7. Alternatively, deviation of biotite chemistry from the pure phlogopite-annite solid-solution would stabilize annite to higher  $f_{\text{O}_2}$ - $f_{\text{S}_2}$ . Biotites in BHE4 and BHE15 contain significant Ti and Al in excess of  $\text{KFe}_3\text{AlSi}_3\text{O}_{10}$  to account for the discrepancy between observed and calculated  $X_{\text{Fe}}$  values.

The composition of phlogopite in BHRAD4 is not constrained by the opaque mineral assemblages because both magnetite and pyrite are absent. Extreme iron depletion reflects the abundance of sulfides in the rock which fix most of the iron leaving the silicate and oxide minerals Mg-enriched.

### Genesis of Host Rock

Lindgren (1925) proposed a process of contact metamorphism-related magnesium metasomatism for the origin of the cordierite-anthophyllite rocks of Blue Hill. However, the association of cordierite-anthophyllite rocks with metamorphosed sedimentary rocks containing stratiform base-metal deposits suggested a genetic link between the mineralization and the magnesium-enrichment in the enclosing sediments. Vallance (1967) suggests cordierite-anthophyllite rocks represent metamorphosed products of hydrothermally altered mafic lavas. Similar hydrothermal processes operating on argillaceous sediments may have produced the requisite quartz-chlorite-illite protolith of the Black Hawk mine cordierite-anthophyllite-bi-

otite rocks. The extreme magnesium and alumina-enriched, silica-depleted rocks associated with the Black Hawk mine ores are isochemical with chlorite or chlorite-talc rocks found in association with unmetamorphosed, stratiform sulfide deposits such as the Harborside deposit (Bouley and Hodder, 1984). Rocks of this unusual bulk composition are also found in unmineralized sedimentary and volcanic terrains but have been interpreted as the result of *in situ* hydrothermal alteration (Warren, 1979). The association of cordierite-anthophyllite and enstatite-spinel-forsterite rocks with stratiform mineralization at Blue Hill suggests they owe their origin to the same submarine hydrothermal activity responsible for the metal deposition.

## CONCLUSIONS

The metamorphic mineral assemblages and associated stratiform Zn-Cu-Pb ores at the Black Hawk mine show the effects of contact metamorphism coincident with the intrusion of the Sedgwick pluton into the Ellsworth Schist. Andalusite-cordierite and cordierite-anthophyllite parageneses are consistent with shallow metamorphic conditions. Pressure is bracketed by the upper stability of andalusite ( $\leq 3.76$  kbar or 376 MPa) and the presence of enstatite, spinel, and forsterite as a chlorite breakdown assemblage ( $> 2.3$  kbar or 230 MPa). The dominance of andalusite and development of fibrolitic sillimanite in orthoclase suggest temperatures in the 500-600°C range. High temperature enstatite-spinel-forsterite assemblages in Mg-rich, silica-deficient rocks and orthoclase-sillimanite paragenesis may be stabilized to lower temperatures by low  $P_{H_2O}$  conditions.

The metamorphic assemblages in rocks surrounding the Black Hawk mine deposit are depleted in FeO and enriched in MgO and  $Al_2O_3$  relative to normal pelitic schists in the Ellsworth Schist. These unusual bulk compositions are due to the combined effects of metamorphism in the presence of a stratiform ore deposit with its accompanying high  $fO_2$  and  $fS_2$  and hydrothermal alteration of the protolith during mineralization.

## ACKNOWLEDGEMENTS

This manuscript greatly benefited from conversations with former Black Hawk mine personnel Jim Pearson and Paul LaPierre and from conversations with Fred Beck. Thanks are also extended to Diane Vane for assistance in preparation of figures and David Stewart and Edward Grew for thoughtful and constructive reviews.

- BACHINSKI, D.J. 1976. Metamorphism of cupriferous iron sulfide deposits, Notre Dame Bay, Newfoundland. *Economic Geology*, 71, pp. 443-452.
- BENCE, A.E. and ALBEE, A.L. 1968. Empirical correction factors for the electron microanalysis of silicates and oxides. *Journal of Geology*, 76, pp. 382-403.
- BERMAN, R.G., ENGI, M., GREENWOOD, H.J., and BROWN, T.H. 1986. Derivation of internally consistent thermodynamic data by the technique of mathematical programming: a review with application to the system MgO-SiO<sub>2</sub>-H<sub>2</sub>O. *Journal of Petrology*, 27, pp. 1331-1364.
- BLÜMEL, P. and PROPACH, G. 1978. Anthophyllite gneiss from the

- Silberberg Fe-sulfide deposit in high-grade metasediments near Bodenmais, E-Bavaria. *Neues Jahrbuch Für Mineralogie Abhandlungen*, 134, pp. 24-32.
- BOULEY, B.A. 1978. Volcanic stratigraphy, stratabound sulfide deposits, and relative age relationships in the east Penobscot Bay area, Maine. Unpublished Ph.D. thesis, University of Western Ontario, 168 p.
- BOULEY, B.A. and HODDER, R.W. 1984. Strata-bound massive sulfide deposits in Silurian-Devonian volcanic rocks at Harborside, Maine. *Economic Geology*, 79, pp. 1693-1702.
- CHENEY, E.S. 1969. Geology of the Blue Hill-Castine mining district, southwestern Hancock County, Maine. Second Annual Report for Maine Geological Survey, 148 p.
- CHERNOSKY, J.V., JR. 1978. The stability of clinocllore + quartz at low pressure. *American Mineralogist*, 63, pp. 73-82.
- DEB, M. 1980. Genesis and metamorphism of two stratiform massive sulfide deposits at Ambaji and Deri in the Precambrian of western India. *Economic Geology*, 75, pp. 572-591.
- EMMONS, W.H. 1909. Some regionally metamorphosed ore deposits and so-called segregated veins. *Economic Geology*, 4, pp. 755-781.
- . 1910. Some ore deposits in Maine and the Milan Mine in New Hampshire. United States Geological Survey, Bulletin 432, 60 p.
- FAWCETT, J.J. and YODER, H.S., JR. 1966. Phase relationships of chlorites in the system MgO-Al<sub>2</sub>O<sub>3</sub>-SiO<sub>2</sub>-H<sub>2</sub>O. *American Mineralogist*, 51, pp. 353-380.
- FLEMING, P.D. and FAWCETT, J.J. 1976. Upper stability of chlorite + quartz in the system MgO-FeO-Al<sub>2</sub>O<sub>3</sub>-SiO<sub>2</sub>-H<sub>2</sub>O at 2 kbars water pressure. *American Mineralogist*, 61, pp. 1175-1193.
- FROESE, E. 1969. Metamorphic rocks from the Coronation Mine and surrounding area. Geological Survey of Canada, Paper 68-5, pp. 55-77.
- . 1971. The graphical representation of sulfide-silicate phase equilibria. *Economic Geology*, 66, pp. 335-341.
- . 1976. Applications of thermodynamics in metamorphic petrology. Geological Survey of Canada, Paper 75-43, 34 p.
- FROESE, E. and GUNTER, A.E. 1976. A note on the pyrrhotite-sulfur vapor equilibrium. *Economic Geology*, 71, pp. 1589-1594.
- FROST, B.R. 1975. Contact metamorphism of serpentinite, chloritic blackwall, and rodingite at Paddy-Go-Easy Pass, Central Cascades, Washington. *Journal of Petrology*, 16, pp. 272-313.
- . 1976. Limits to the assemblage forsterite-anorthite as inferred from peridotite hornfels, Icicle Creek, Washington. *American Mineralogist*, 61, pp. 732-750.
- GILLSON, J.L. and WILLIAMS, R.S. 1929. Contact metamorphism of the Ellsworth Schist near Blue Hill, Maine. *Economic Geology*, 24, pp. 182-194.
- GREW, E.S. 1988. Korerupine at the Sar-e-Sang, Afghanistan, whiteschist locality: implications for tourmaline-korerupine distribution in metamorphic rocks. *American Mineralogist*, 73, pp. 345-357.
- GUIDOTTI, C.V. 1970. The mineralogy and petrology of the transition from the lower to the upper sillimanite zone in the Oquossoc area, Maine. *Journal of Petrology*, 11, pp. 277-336.
- HAWTHORNE, F.C. 1981. Crystal chemistry of amphiboles. In *Amphiboles and other hydrous pyriboles - mineralogy*. Edited by P.H. Ribbe. Mineralogical Society of America, Reviews in Mineralogy, 9A, pp. 1-104.
- HOLDAWAY, M.J. 1971. Stability of Andalusite and the aluminum silicate phase diagram. *American Journal of Science*, 271, pp. 97-131.
- HOLDAWAY, M.J. and LEE, S.M. 1977. Fe-Mg cordierite stability in

- high-grade pelitic rocks based on experimental, theoretical, and natural observations. *Contributions to Mineralogy and Petrology*, 63, pp. 175-188.
- HOWD, F.H. and DRAKE, D.P. 1974. Economic deposits at Blue Hill. *In Geology of East-Central and North-Central Maine*, New England Intercollegiate Geological Conference Guidebook, 1974. *Edited by Osberg*. Pp. 180-189.
- KINKEL, A.R. 1967. The Ore Knob copper deposit North Carolina, and other massive sulfide deposits of the Appalachians. United States Geological Survey, Professional Paper 558, 58 p.
- LAL, R.K. and MOOREHOUSE, W.W. 1969. Cordierite-gedrite rocks and associated gneisses of Fishtail Lake, Harcourt Township, Ontario. *Canadian Journal of Earth Science*, 6, pp. 145-165.
- LAPIERRE, P.T. 1978. The geology, zoning, and textural features of the Second Pond ore deposit, Blue Hill, Maine. Unpublished Masters thesis, University of Maine, 75 p.
- LI, C. 1942. Genesis of some ore deposits in southeastern Maine. *Geological Society of America Bulletin*, 53, pp. 15-51.
- LINDGREN, W. 1925. The cordierite-anthophyllite mineralization at Blue Hill, Maine, and its relation to similar occurrences. *National Academy of Sciences, Proceedings*, 2, pp. 1-4.
- NESBITT, B.E. 1986. Oxide-sulfide-silicate equilibria associated with metamorphosed ore deposits, part II: Pelitic and felsic volcanic terrains. *Economic Geology*, 81, pp. 841-856.
- NEWHOUSE, W.H. and FLAHERTY, G.F. 1930. The texture and origin of some banded or schistose sulphide ores. *Economic Geology*, 25, pp. 600-620.
- PERKINS, E.H., BROWN, T.H., BERMAN, R.G. 1986. PTX-SYSTEM: three programs for calculation of pressure-temperature-composition phase diagrams. *Computers and Geosciences*, 12, pp. 749-755.
- ROBIE, R.A., HEMINGWAY, B.S., and FISHER, J.R. 1978. Thermodynamic properties of minerals and related substances at 298.15 K and 1 bar (105 Pascals) pressure and at higher temperatures. U.S. Geological Survey, Bulletin 1452, 456 p.
- SLAUGHTER, J., KERRICK, D.M., and WALL, J.V. 1975. Experimental and thermodynamic study of equilibria in the system CaO-MgO-SiO<sub>2</sub>-H<sub>2</sub>O-CO<sub>2</sub>. *American Journal of Science*, 275, pp. 143-162.
- STEWART, D.B. and WONES, W.R. 1974. Bedrock geology of northern Penobscot Bay area. *In Geology of East-Central and North-Central Maine*, New England Intercollegiate Geological Conference Guidebook, 1974. *Edited by Osberg*. Pp. 223-239.
- TAYLOR, B.E. and SLACK, J.F. 1984. Tourmalines from Appalachian-Caledonian massive sulfide deposits: textural, chemical, and isotopic relationships. *Economic Geology*, 79, pp. 1703-1726.
- THOMPSON, J.B., JR. 1972. Oxides and sulfides in regional metamorphism of pelitic schists. 24th International Geological Congress, Section 10, pp. 27-35.
- TOULMIN, P. and BARTON, P.B. 1964. A thermodynamic study of pyrite and pyrrhotite. *Geochemica et Cosmochimica Acta*, 28, pp. 641-671.
- UPADHYAY, H.D. and SMITHERINGALE, W.G. 1972. Geology of the Gullbridge copper deposit, Newfoundland: volcanogenic sulfides in cordierite-anthophyllite rocks. *Canadian Journal of Earth Science*, 9, pp. 1061-1073.
- VALLANCE, T.G. 1967. Mafic rock alteration and the isochemical development of cordierite anthophyllite rocks. *Journal of Petrology*, 8, pp. 84-96.
- WARREN, R.G. 1979. Sapphirine-bearing rocks with sedimentary and volcanogenic protoliths from the Arunta Block. *Nature*, 278, pp. 159-161.
- WOLTER, H.U. and SEIFERT, F. 1984. Mineralogy and genesis of cordierite-anthophyllite rocks from the sulfide deposit of Falun, Sweden. *Lithos*, 17, pp. 147-152.